

# Modeling the Effect of Nail Corrosion on the Lateral Strength of Joints

Samuel L. Zelinka  
Douglas R. Rammer

---

## Abstract

This article describes a theoretical method of linking fastener corrosion in wood connections to potential reduction in lateral shear strength. It builds upon published quantitative data of corrosion rates of metals in contact with treated wood for several different wood preservatives. These corrosion rates are then combined with yield theory equations to calculate a loss in lateral capacity as a function of time. The calculations are straightforward and can be performed in a spreadsheet or simple computer program. They can accommodate time-dependent and moisture-dependent corrosion rates. The latter of these capabilities can easily be recognized as important, inasmuch as corrosion rates of fasteners are recognized as being dependent on moisture content of the wood in which they are embedded. The calculation method is dependent on corrosion rate, and the method is therefore limited by the lack of agreement in corrosion rates presented in the literature. Within these limitations, the article examines how different corrosion rates and changes in corrosion rates affect the mechanical properties and service life of nailed wood joints.

---

Since the voluntary withdrawal of chromated copper arsenate (CCA) as a wood preservative for residential construction in January 2004, the corrosion of metals in contact with preservative-treated wood has been a research emphasis. In addition to numerous articles on the mechanism of corrosion in treated wood (e.g., Kear et al. 2009; Zelinka et al. 2010; Zelinka and Stone 2010, 2011), a standard has also been developed to measure the corrosion rates of metals embedded in treated wood (ASTM International 2011). The emphasis of corrosion research has been on quantifying the metal corrosion rate in units of depth of metal wastage per unit of time. The previous work represents a significant improvement in the understanding of how metals in wood corrode. However, because metals in wood are used to fasten two wooden members together, the loss in joint strength with time is just as important as the amount of metal that has corroded. Nguyen et al. (2011) have highlighted the importance of incorporating corrosion into a reliability-based timber engineering design code and proposed a preliminary model to do so based upon time of wetness for untreated and CCA-treated wood.

This article extends previous work on the degradation of wood-metal connections by examining how metal corrosion leads to a loss of structural capacity of a laterally loaded nailed joint. The reduction in lateral capacity is calculated from yield theory equations given in the “National Design Specification (NDS) for Wood Construction” (American Wood Council 2012). Specific examples are shown comparing the reduction in lateral capacity as a function

of time for corrosion rates measured for untreated, alkaline copper quaternary (ACQ)-treated, and CCA-treated wood.

## Method for Calculating the Loss of Lateral Capacity

### Yield theory equations

Single-fastener connection performance is dependent on joint geometry, fastener diameter, dowel bending-yield strength, dowel bearing strength, and direction of load to the grain. Yield expressions relating these parameters were developed by Johansen (1949) using a static analysis that assumes the wood and the metal dowel fastener are both perfectly plastic. After nearly a decade of development, the yield model became the standard for dowel connection design in the 1991 NDS and is applicable to all types of dowel fasteners—nails, lag screws, and bolts (McLain and Thangjitham 1983, Aune and Patton-Mallory 1986, Soltis et al. 1986, Soltis and Wilkinson 1987, McLain 1992, Wilkinson 1993). The yield theory model selects the worst case of yield modes based on different possibilities of wood bearing and nail bending.

---

The authors are, respectively, Materials Research Engineer and Research General Engineer, USDA Forest Serv., Forest Products Lab., Madison, Wisconsin (szelinka@fs.fed.us [corresponding author], drammer@fs.fed.us). This paper was received for publication in August 2011. Article no. 11-00105.

©Forest Products Society 2012.  
Forest Prod. J. 62(3):160–166.

Mode I is a wood-bearing failure in either the main or side member, Mode II is a rotation of the fastener in the joint without bending, and Modes III and IV are a combination of wood-bearing failure and one or more plastic hinge yield formations in the fastener. In addition to yield modes, we have included the transverse shear of the fastener as a possible failure mode. For a two-member nailed joint, the lateral design load  $Z(N)$  of a joint is determined by the minimum of the following yield expressions because a Mode II failure is not expected for smaller diameter fasteners such as nails:

$$Z = \min \left\{ \begin{array}{ll} \frac{DT_s F_{es}}{2.2} & \text{(Mode I}_s\text{)} \\ \frac{k_2 D l_p F_{em}}{2.2(1 + 2R_e)} & \text{(Mode III}_m\text{)} \\ \frac{k_3 D T_s F_{em}}{2.2(2 + R_e)} & \text{(Mode III}_s\text{)} \\ \frac{D^2}{2.2} \sqrt{\frac{2F_{em} F_{yb}}{3(1 + R_e)}} & \text{(Mode IV)} \\ \frac{3\pi d^2}{16} (F_v) & \text{(Fastener shear)} \end{array} \right. \quad (1)$$

where

$$\begin{aligned} k_2 &= -1 + \sqrt{2(1 + R_e) + \frac{2F_{yb}(1 + 2R_e)D^2}{3F_{em}l_p^2}} \\ k_3 &= -1 + \sqrt{\frac{2(1 + R_e)}{R_e} + \frac{2F_{yb}(2 + R_e)D^2}{3F_{em}T_s^2}} \\ R_e &= F_{em}/F_{es} \quad \text{and} \\ F_v &= \frac{F_{yb}}{\sqrt{3}} \end{aligned} \quad (2)$$

and where  $D$  is the dowel diameter (mm),  $F$  is the dowel bearing stress of the main ( $F_{em}$ ) or side ( $F_{es}$ ) member (MPa),  $F_{yb}$  is the bending-yield stress of the nail (MPa),  $l_p$  is the length of penetration into the main member, and  $T_s$  is the thickness of the side member. For a shear failure, the yield shear stress is determined from  $F_{yb}$  because pure shear occurs on  $45^\circ$  planes, and  $F_{yb}$  is representative of the material tensile yield stress for a fully plastic section.

In the following examples illustrating the effect of corrosion on the lateral fastener strength, several assumptions were made. The first assumption is that the corrosion only reduces the section modulus of the nail, not  $F_{yb}$  or the elastic modulus of the fastener. Practically, this assumption is implemented also assuming uniform corrosion over the entire nail and using the corrosion rate as a constant reduction in diameter with time. The other assumptions deal with the dowel bearing strength. It is assumed that the corrosion by-products do not affect  $F_e$  and that at failure, the wood moisture content is greater than 19 percent; in this regime, the NDS treats dowel bearing strength as independent of moisture content (Rammer 2001). This is reasonable because it is likely that the moisture content is greater than 19 percent if corrosion is occurring (Baker 1988, Short and Dennis 1997).

For a given joint geometry, wood species, and fastener bending-yield stress, the equations depend only on the fastener diameter, which is a function of the corrosion rate. Corrosion rates for metals in wood will be reviewed in the following section. These corrosion rates will then be used throughout the article to examine the relative lateral capacity of nailed joints in many different scenarios.

### Corrosion rates of metals in contact with treated wood

Since the voluntary withdrawal of CCA for use in residential construction, many experiments have measured the corrosion of metals in ACQ- and CCA-treated wood (Freeman and McIntyre 2008, Zelinka et al. 2008, Kear et al. 2009, Zelinka and Rammer 2009). However, there is little agreement between these measurements; the measured corrosion rates from these tests have a wide range of values, for example, from 2 to 113  $\mu\text{m y}^{-1}$  and from 1 to 26  $\mu\text{m y}^{-1}$  for hot-dip galvanized steel in ACQ- and CCA-treated wood, respectively. These wide differences in measured corrosion rates most likely result from experimental differences in temperature, relative humidity, and wood moisture content. The emphasis of this article is on the framework for analyzing how the relative lateral capacity depends upon corrosion rate; therefore, only a few representative corrosion rates will be used in the ensuing analysis. The representative condition chosen for further analysis is  $27^\circ\text{C}$ , 100 percent relative humidity (RH), which Baechler (1949) chose to simulate outdoor exposures. The condition is chosen because data exist under these conditions for hot-dip galvanized steel in untreated and CCA-treated and ACQ-treated wood, and it is one of the most tested environments for wood-metal corrosion (Baechler 1949, Baker 1992, Kear et al. 2009, Zelinka and Rammer 2009, Zelinka et al. 2010).

The corrosion rate for CCA-treated wood comes from a study conducted by Baker (1992), which reported the percent weight loss for “CCA-I” and “CCA-II,” which were essentially equivalent to modern CCA-A and CCA-B. Zelinka and Rammer (2009) later converted the percent weight loss to a true corrosion rate. Baker’s study involved 11 different types of metal fasteners embedded in CCA-treated and ammoniacal copper arsenate (ACA)-treated wood at  $27^\circ\text{C}$  and 97 to 100 percent RH for periods of 1, 3, and 14 years. Baker found a linear relationship between percent weight loss and time, which implies a constant corrosion rate assuming a constant surface area. The corrosion rate for CCA-I, which was found constant between 1 and 14 years, is used in the remainder of this article (Table 1).

The untreated and ACQ-treated wood corrosion rates come from 1-year exposure tests at  $27^\circ\text{C}$  and 100 percent RH (Zelinka and Rammer 2009, Zelinka et al. 2010). These corrosion rates are assumed to be constant with time, as was observed by Baker in CCA-I-treated wood. This assumption and its implications are further examined in the section “Examination of a time-dependent corrosion rate.”

The corrosion rates, treatments, and original source for the data are summarized in Table 1 and will be referred to throughout the article.

### Effect of Corrosion on the Lateral Joint Strength

To illustrate how the yield theory equations can be used to calculate the reduction in lateral joint strength, we examine

Table 1.—Corrosion rates used in this study and pertinent details from the original study.<sup>a</sup>

Corrosion rate ( $\mu\text{m y}^{-1}$ )	Reference	Treatment	Experimental details
5	Zelinka et al. (2010)	Untreated	1-y exposure in a desiccator maintained at 27°C, 100% RH
10	Baker (1992), Zelinka and Rammer (2009)	9.6 kg/m <sup>3</sup> CCA-I <sup>b</sup>	1, 3, and 14 y in an enclosure at 27°C with a humidifier to maintain 97%–100% RH
60	Zelinka and Rammer (2009)	4 kg/m <sup>3</sup> ACQ-D <sup>c</sup>	1-y exposure in a desiccator maintained at 27°C, 100% RH

<sup>a</sup> All tests were performed on hot-dip galvanized steel fasteners. RH = relative humidity.

<sup>b</sup> CCA = chromated copper arsenate. CCA-I was a formulation of CCA listed in an outdated classification system. CCA-I was essentially equivalent to CCA-A (“salt” formulation of CCA). CCA-A imparted greater conductivity to wood treated with it than does CCA-C (Richards 1990). CCA-C is the only CCA formulation currently listed in American Wood-Preservers’ Association standards. CCA-C has retained Environmental Protection Agency listing as a restricted use preservative (Lebow 2010).

<sup>c</sup> ACQ = alkaline copper quaternary.

the corrosion of an 8d common nail (length, 63 mm;  $D = 3.4$  mm) in treated southern pine (*Pinus* spp;  $F_{yb} = 620$  MPa,  $F_{em} = F_{es} = 38$  MPa). We first illustrate how these equations can be used to predict the loss in lateral strength with time for all yield theory modes. We then focus on Mode IV yielding and show the percentage of the original capacity as a function of time. If an arbitrary failure criterion (e.g., 50% of original capacity) were defined, the time to failure could be determined with these data. To illustrate the flexibility and robustness of this methodology, three additional cases are examined. In the first case, a coated fastener is examined. The final two cases examine what happens when the corrosion rate varies with time and moisture content.

### Examination of all failure modes

Figure 1 presents the reduction in capacity of the lateral strength of a single shear nailed joint for corrosion rates of  $10 \mu\text{m y}^{-1}$  (Fig. 1a) and  $60 \mu\text{m y}^{-1}$  (Fig. 1b). These corrosion rates are roughly equivalent to those measured in exposure tests for hot-dip zinc galvanized fasteners in CCA- and ACQ-treated wood, respectively (Table 1). Each line on the graph represents a 10 percent reduction in capacity, and the second order discontinuities are a result of a change in failure mode. For a narrow side member, which exhibits Mode I behavior, the reduction is directly related to the

reduction of nail diameter due to corrosion. As the side member thickness increases, the reduced diameter will affect both the bearing and nail bending performance. For large enough side member thicknesses, the joints will fail in Mode IV, which is independent of the wood thicknesses. Transverse fastener shear is never the controlling failure mechanism. Importantly, joints governed by Mode IV have the fastest reduction in capacity with time. Because most of the work on corrosion in wood has examined decking nails, and the most common decking material in the United States is “5/4 radial deck board” (25 mm thick), it can be expected that decking nails will most likely exhibit a Mode IV yielding in service. Not only does a Mode IV failure represent the most probable failure mode in decking applications but it also represents the quickest time to complete strength loss. Therefore, only Mode IV failures will be considered in the next four cases.

### Examination of Mode IV yield mode

For Mode IV failures, which are expected in decking applications, the reduction in lateral capacity depends only upon the corrosion rate and the initial diameter of the fastener. Figure 2 illustrates the reduction in lateral capacity for an 8d nail in a Mode IV failure with several different corrosion rates. The  $5\text{-}\mu\text{m y}^{-1}$  corrosion rate corresponds to

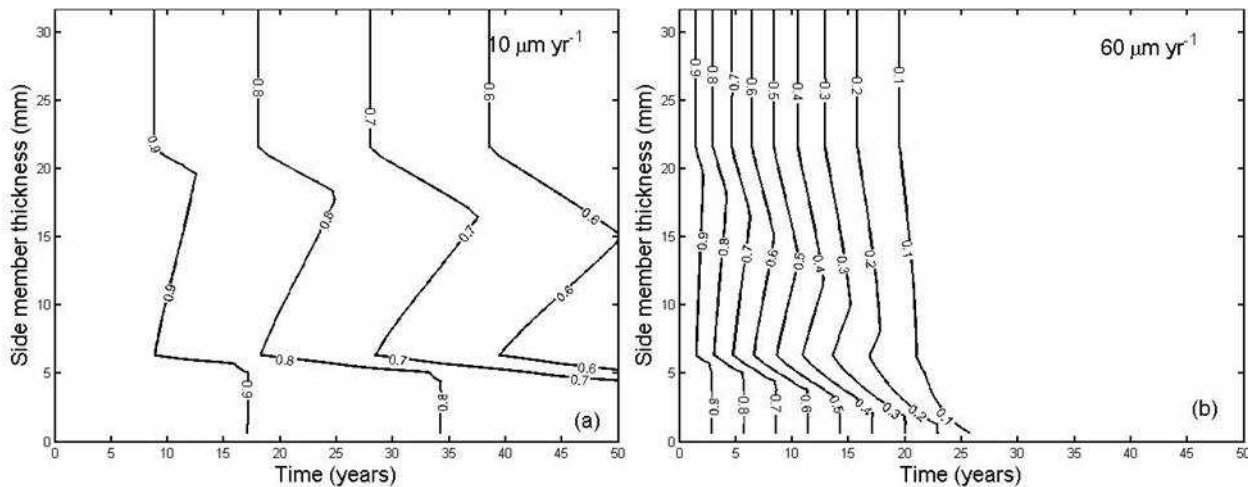


Figure 1.—Percent reduction of capacity as a function of time for an 8d common (3.4-mm) fastener embedded in wood with an assumed corrosion rate of (a)  $10 \mu\text{m y}^{-1}$  or (b)  $60 \mu\text{m y}^{-1}$ , which corresponds to corrosion rates measured for hot-dip galvanized steel at 27°C, 100 percent relative humidity for chromated copper arsenate- and alkaline copper quaternary-treated wood, respectively. Each contour represents a 10 percent loss in capacity.

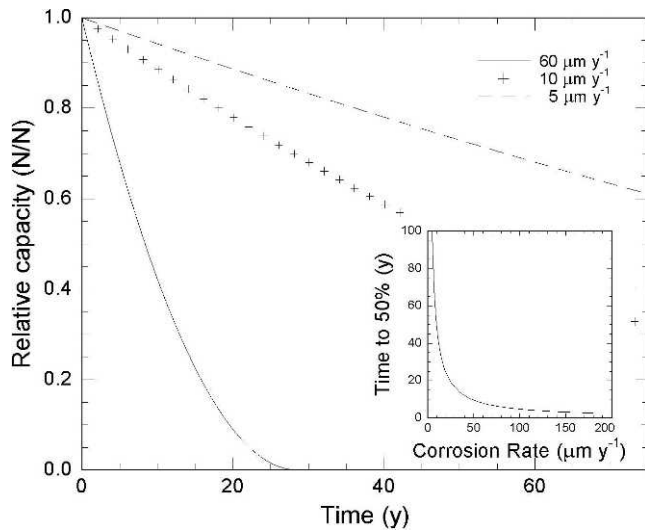


Figure 2.—Reduction in capacity of an 8d decking nail exhibiting a Mode IV failure. (Inset) The number of years until a 50 percent reduction in capacity is reached as a function of corrosion rate.

galvanized steel in untreated wood, and the 10 and 60  $\mu\text{m y}^{-1}$  corrosion rates have been described previously (Table 1). For Mode IV failures, the yield strength is inversely related to the square of the diameter, which results in the lateral capacity decreasing rapidly with increasing corrosion rate. By arranging the terms, it is possible to express the time to a given percentage of the original capacity as a function of the corrosion rate,  $r$ , and the original diameter,  $d_0$ . For instance, the time to 50 percent of the original capacity,  $t_{50}$ , can be given by

$$t_{50} = \frac{d_0(2 - \sqrt{2})}{4r} \quad (3)$$

This expression is shown graphically for an 8d fastener in the inset of Figure 2.

### Examination of a galvanized fastener

For galvanized and other metal-coated fasteners, corrosion rate in the initial stages, when the coating is continuous and completely intact, is equivalent to the corrosion rate of the coating metal by itself. Once the coating has completely corroded away, corrosion proceeds at the rate of the base metal. The measured corrosion rates (Table 1) are high enough that a typical hot-dip galvanized fastener (with a coating on the order of 100  $\mu\text{m}$ ) would last only a few years before the base metal was completely exposed. Therefore, it is instructive to examine how the above calculations change for coated fasteners, where the corrosion rate experiences a change when the coating has disappeared, that is,

$$r = \begin{cases} r_{\text{coat}} & 0 < t < t_{\text{crit}} \\ r_{\text{base}} & t > t_{\text{crit}} \end{cases} \quad (4)$$

where  $t_{\text{crit}}$  is the time at which the galvanized coating has completely corroded away, given by

$$t_{\text{crit}} = \frac{T_{\text{coat}}}{r_{\text{coat}}} \quad (5)$$

where  $T_{\text{coat}}$  is the thickness of the coating. Although

Equation 4 is generally valid, literature values on the ratio of corrosion rates of galvanized steel to plain steel corrosion rates in treated wood vary greatly. Kear et al. (2009) and Zelinka et al. (2010) both measured the corrosion of metals embedded in wood for 1 year in an environmental chamber at 100 percent RH. Surprisingly, Kear et al. observed that the corrosion rate of galvanized steel was less than that of plain steel, whereas Zelinka observed that the corrosion rate of galvanized steel was greater than that of plain steel.

Given this uncertainty in relative corrosion rates, it is possible that the corrosion rate of a galvanized fastener could increase or decrease once the coating has completely corroded. In either case, the relative lateral capacity as a function of time will depend upon the corrosion rates of both the coating and base metal. The total loss in capacity can be determined by Equations 4 and 1. Figure 3 illustrates the importance of accounting for the corrosion rate of the coating for an 8d nail exhibiting a Mode IV failure, where the galvanized coating is 100- $\mu\text{m}$  thick and has a corrosion rate of 10  $\mu\text{m y}^{-1}$  (CCA-I; Table 1). Along with the “baseline case” where the entire thickness of the fastener has the same corrosion rate, two different scenarios are plotted. In the first case, the ratio of the steel corrosion rate to the galvanized corrosion rate is assumed to be 2.5, as found by Kear et al. (2009); in the second, it is assumed to be 0.5, as found by Zelinka et al. (2010). It is clear from Figure 3 that the corrosion rate of the base metal plays an important role in the reduction in capacity of the structure with time because the coating can be completely corroded so quickly.

### Examination of a time-dependent corrosion rate

The above analysis assumes that the corrosion rate is constant with time, which is consistent with observations by Baker (1992) for galvanized fasteners embedded in treated wood for times ranging between 1 and 14 years. This is consistent with literature observations of the corrosion rate of galvanized steel exposed to atmospheric corrosion;

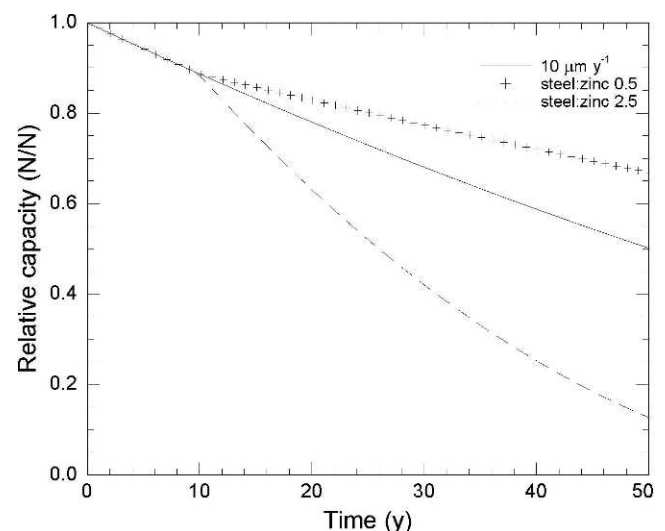


Figure 3.—Relative capacity as a function of time for an 8d common galvanized fastener corroding at 10  $\mu\text{m y}^{-1}$  and exhibiting a Mode IV failure. Different lines represent different relative steel:galvanized steel corrosion rate ratios.

Legault and Pearson (1978) reviewed the corrosion kinetics of galvanized steel and found that in most industrial and marine environments, galvanized steel exhibited a constant corrosion rate because the corrosion products dissolve in low-pH water/rainwater. Because it is well known that wood is acidic, it is not surprising that galvanized steel exhibits a constant corrosion rate in wood. However, for most other metals, and for galvanized steel exposed to less acidic conditions, the corrosion rate usually decreases with time (Zhang 2003).

Empirically, it has been observed that the corrosion kinetics for atmospheric corrosion can be described by

$$\Delta W = Kt^n \quad (6)$$

where  $\Delta W$  is the change in weight,  $K$  is a constant (the 1-y corrosion rate),  $t$  is the time in years, and  $n$  is an exponent that controls the kinetics and describes the resistance for ion transport to the metal surface through the corrosion product once it has formed. The limiting case,  $n = 1$ , observed by Baker (1992), corresponds with a constant corrosion rate with time and physically represents a case where the corrosion products do not remain on the surface, or they remain but do not decrease the rate of corrosion. In theory,  $n = 0.5$  should represent the lower bound, where the reaction is limited by the diffusion of ions to the metal surface. However, values of  $n$  as low as 0.36 have been observed in carbon steels exposed to atmospheric conditions (Legault and Preban 1975).

Although the data suggest that metals in wood exhibit a constant corrosion rate with time (i.e.,  $n = 1$ ), only one article examined this behavior (Baker 1992). It is possible that the corrosion rate is not constant but rather changes with time. If the commonly accepted atmospheric corrosion kinetic model holds for wood, the  $n = 1$  case represents a worst-case scenario.<sup>1</sup> By combining Equation 6 with the yield theory equations (Eq. 1), it is possible to examine how a decreasing corrosion rate would affect the relative lateral capacity of nailed joints. Figure 4 examines the same case as Figure 2 with a time-dependent corrosion rate (i.e., the 60- $\mu\text{m y}^{-1}$  curve in Fig. 2 is equivalent to the  $n = 1$  case in Fig. 4). The values of  $n$  were selected to be representative of those observed for different classes of materials as observed by Legault and Preban (1975), and the corrosion rate as a function of time is shown as an inset. Any change in  $n$  represents not only a decrease in the corrosion rate but also a deceleration with time and therefore has a large effect on the relative capacity with time.

### Examination of a moisture-dependent corrosion rate

The wood moisture content is the most important environmental variable to the corrosion of metals embedded in wood. Below 15 to 18 percent moisture content, embedded metals do not corrode (Baker 1988, Short and Dennis 1997). Above this threshold, the corrosion rate increases with increasing moisture content before eventually reaching a plateau (Short and Dennis 1997, Kear et al.

<sup>1</sup> It is possible but physically unlikely that the corrosion of metals in wood increases with time. In this case, Equation 6 would no longer be applicable and a different kinetic model would need to be developed.

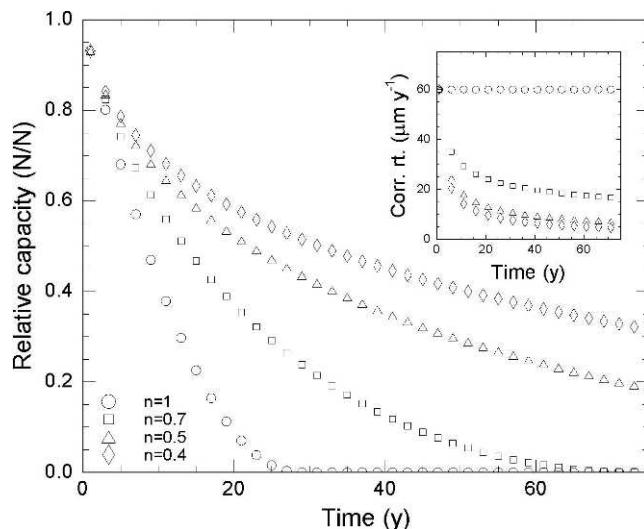


Figure 4.—Relative capacity as a function of time for a Mode IV failure where the corrosion rate decreases with time according to Equation 6. The inset shows how the corrosion rate changes with time for values of  $n$ .

2009). Because of this sensitivity, most laboratory corrosion rate measurements have been under conditions where the wood moisture content is either constant or well characterized (e.g., American Wood-Preservers' Association 2007). However, in actuality, wood exposed to the environment can experience large fluctuations in moisture content (Gaby and Duff 1978, Miller and Boxall 1987, Cui and Zahora 2000). Because of these large fluctuations in moisture content, and the resulting fluctuations in corrosion rate, a steady-state approximation of the corrosion rate can be misleading.

Recently, Zelinka et al. (2011) developed a combined hygrothermal/corrosion model to predict the cumulative corrosion at various points along the length of an embedded fastener as a function of time. The process consists of two steps: the first step is to calculate the wood moisture content profile from hourly climatic data using a hygrothermal model. The second step is to use the moisture content calculated from the hygrothermal model to calculate the metal corrosion rate, which is assumed to be constant over the hour. The hourly amounts of corrosion are summed, resulting in a final output of the depth of the corrosion attack (in micrometers) along the entire length of the fastener. The hygrothermal model uses an existing, validated two-dimensional finite element code to solve the coupled heat and mass transport equations using hourly climatic data as an input (Janssen et al. 2007). It predicts moisture content and temperature at various depths within the wood. In the subsequent calculation of corrosion rate, two simplifying assumptions are made: that corrosion ceases at temperatures below freezing, regardless of moisture content, and that at temperatures above freezing, corrosion rate is solely dependent on moisture content.

The moisture dependence of the corrosion rate was incorporated by fitting the empirical polarization resistance data of Short and Dennis (1997) with

$$R = \frac{A}{1 + e^{B(C-w)}} \quad (7)$$

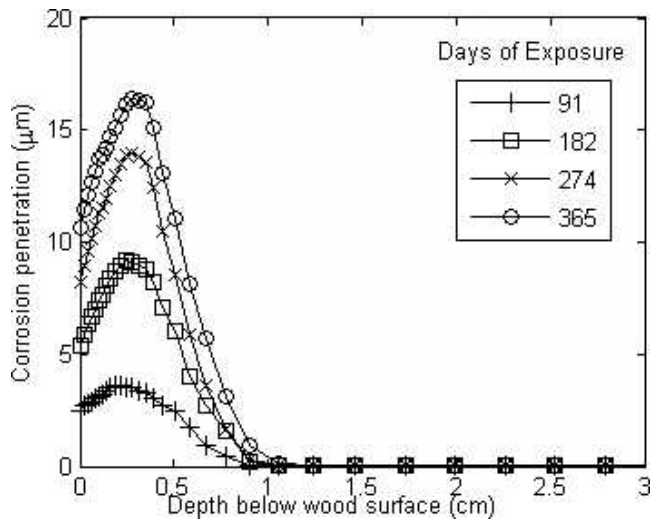


Figure 5.—Output (corrosion profile as a function of time) from the hygrothermal model, based upon climatic data from Baltimore for calendar year 1989.

where  $A$  represents the maximum corrosion rate ( $\mu\text{m y}^{-1}$ ),  $B$  represents the steepness of the transition from 0 to  $A$ ,  $C$  represents the moisture content at which  $R = A/2$ , and changing  $C$  changes the corrosion threshold moisture content. The parameters  $B$  (0.83) and  $C$  (24) are taken from a fit of the published data of Short and Dennis (1997). The parameter  $A$ , which is physically the asymptotic corrosion limit, is taken as  $52.3 \mu\text{m y}^{-1}$  from recent electrochemical measurements of hot-dip galvanized steel in an extract of ACQ-treated southern pine (Zelinka et al. 2008).

The result of these simulations is the corrosion profile—the depth of corrosion penetration into the nail shank as a function of position along the length of the nail and of time. Results from a 1-year simulation for a specific reference year<sup>2</sup> in Baltimore, Maryland, are included in Figure 5. As Figure 5 shows, the maximum amount of corrosion occurs 0.18 cm below the surface, and the corrosion profile changes throughout the year. This is consistent with empirical observations of corroded fasteners (Kubler 1992). The combined hygrothermal/corrosion model illustrates how fluctuations in moisture content affect the corrosion of embedded fasteners, and the model can be extended using Equation 1 to predict the loss in capacity as a function of time.

To illustrate the importance of moisture fluctuations on the corrosion and the resulting loss in lateral capacity, Figure 6 was created based upon the 1-year simulation for Baltimore (Fig. 5). The analysis uses the same assumptions as Figure 2, but the corrosion rate is calculated from Equation 5. Although the moisture content (and therefore the corrosion rate) depends upon the depth below the surface (Fig. 5), the analysis assumes a worst-case scenario and uses the moisture content at 0.18 cm. Two scenarios are presented in the figure—the first assumes a constant corrosion rate based upon the yearly mean moisture content

<sup>2</sup> The reference year was 1989. This year was chosen on the basis of being the 10th percentile year in terms of number of hours of precipitation from 1960 to 1990. For further discussion of the choice of reference years see Zelinka et al. (2011).

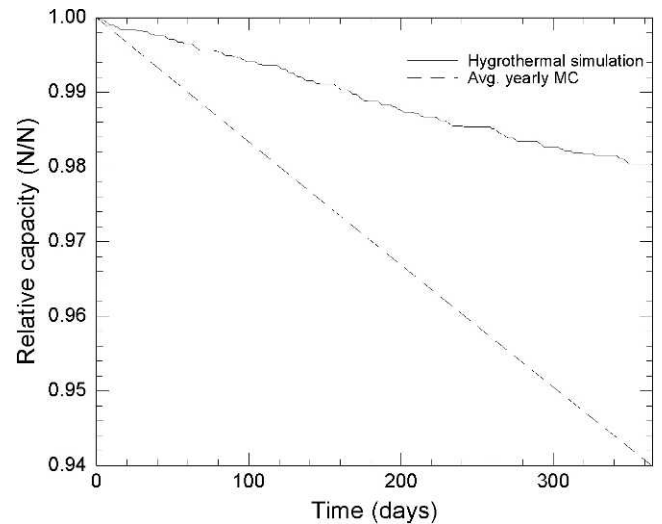


Figure 6.—Relative capacity as a function of time (same parameters as Fig. 2) for two cases, based on the yearly average moisture content, or based on the instantaneous moisture content from a hygrothermal simulation.

(33%), and the second uses a different corrosion rate for every hourly output of the simulation. The two analyses give quite different results. This is most likely a result of the highly nonlinear shape of Equation 5, which is nearly a Heaviside function. Because the yearly average moisture content was greater than  $C$ , the assumed corrosion rate was higher than the average of the hourly corrosion rate data. Although the average annual moisture content overestimated the amount of predicted corrosion, it should give a conservative bound for design in most cases.

## Summary and Conclusions

Although the corrosion rates of metals embedded in treated wood are small in absolute terms, this work has shown that fastener corrosion can have a large effect on the lateral strength of nailed joints in outdoor structures. Although the major aim of the article was to present a methodology for practicing engineers to make informed design decisions for specific wood–metal combinations, several interesting conclusions can be drawn from the scenarios examined in this article:

- In most decking applications, a Mode IV yielding of the fastener is expected. In this case the lateral capacity is proportional to the square of the fastener diameter, resulting in the most rapid time to failure (Fig. 1). If “failure” is defined as an arbitrary percentage of the original capacity, the time to failure is proportional to the reciprocal of the corrosion rate (Fig. 2).
- For galvanized fasteners, the measured corrosion rates suggest that the coating will be completely corroded within a few years. If the base metal has a different corrosion rate than the coating, this results in a large change in the reduction of capacity as a function of time (Fig. 3).
- Only a few measurements have examined the corrosion rate of zinc in treated wood as a function of time. The results from the most comprehensive study (Baker 1992) are consistent with a constant, time-invariant, corrosion rate. If the corrosion rate decreased with time, this would

drastically increase the service life of fasteners (Fig. 4). If the kinetics are indeed consistent with Equation 6, a constant corrosion rate assumption gives a conservative service life estimation.

- Hygrothermal simulations and a moisture-dependent corrosion rate model give practicing engineers tools to make more accurate predictions of the corrosion rate of fasteners in a given structure. Using an average yearly moisture content gives a conservative bound on the residual capacity (Fig. 6).

## Acknowledgments

The authors acknowledge funding from the Federal Highway Administration Covered Bridge Research Program. The authors thank Charles Carll and William J. Feist for constructive feedback.

## Literature Cited

- American Wood Council. 2012. National Design Specification (NDS) for wood construction. 2012 ed. American Wood Council, Leesburg, Virginia.
- American Wood-Preservers' Association (AWPA). 2007. Standard method of determining corrosion of metal in contact with treated wood. AWPA E-12. AWPA, Selma, Alabama.
- ASTM International. 2011. Standard test method for determining the relative corrosion performance of driven fasteners in contact with treated wood. ASTM G198-11. ASTM International, West Conshohocken, Pennsylvania.
- Aune, P. and M. Patton-Mallory. 1986. Lateral load-bearing capacity of nailed joints based on the yield theory: Theoretical development. Research Paper FPL 469. USDA Forest Service, Forest Products Laboratory, Madison, Wisconsin. 20 pp.
- Baechler, R. H. 1949. Corrosion of metal fastenings in zinc-chloride treated wood after 20 years. In: Proceedings of the 45th Annual Meeting of the American Wood-Preservers' Association, St. Louis, Missouri; AWPA, Bethesda, Maryland. pp. 381–397.
- Baker, A. J. 1988. Corrosion of metals in preservative-treated wood. In: Wood Protection Techniques and the Use of Treated Wood in Construction. M. Hamel (Ed.). Forest Products Society, Madison, Wisconsin. pp. 99–101.
- Baker, A. J. 1992. Corrosion of nails in CCA- and ACA-treated wood in two environments. *Forest Prod. J.* 42(9):39–41.
- Cui, F. and A. Zahora. 2000. Effect of a water repellent additive on the performance of ACQ treated decks. IRG/WP 00–40168. In: Proceedings of the 31st Annual Meeting of the International Research Group on Wood Preservation, May 14–19, 2000, Kona, Hawaii; IRG Secretariat, Stockholm.
- Freeman, M. A. and C. R. McIntyre. 2008. A comprehensive review of copper-based wood preservatives with a focus on new micronized or dispersed copper systems. *Forest Prod. J.* 58(11):6–27.
- Gaby, L. I. and J. E. Duff. 1978. Moisture content changes in wood deck and rail components. Research Paper SE-190. USDA Forest Service, Southeastern Forest Experiment Station, Asheville, North Carolina. 12 pp.
- Janssen, H., B. Blocken, and J. Carmeliet. 2007. Conservative modelling of the moisture and heat transfer in building components under atmospheric excitation. *Int. J. Heat Mass Transfer* 50(5–6):1128–1140.
- Johansen, K. W. 1949. Theory of timber connections. *Int. Assoc. Bridge Struct. Eng.* 9:249–262.
- Kear, G., H.-Z. Wu, and M. S. Jones. 2009. Weight loss studies of fastener materials corrosion in contact with timbers treated with copper azole and alkaline copper quaternary compounds. *Corrosion Sci.* 51(2):252–262.
- Kubler, H. 1992. Corrosion of nails in wood construction interfaces. *Forest Prod. J.* 42(1):47–49.
- Lebow, S. T. 2010. Wood preservation, chap. 15. In: Wood Handbook. R. J. Ross (Ed.). General Technical Report FPL-GTR-190.
- Legault, R. A. and V. P. Pearson. 1978. Kinetics of the atmospheric corrosion of galvanized steel. In: Atmospheric Factors Affecting the Corrosion of Engineering Metals. ASTM STP 646. S. K. Coburn (Ed.). American Society for Testing and Materials, West Conshohocken, Pennsylvania. pp. 83–96.
- Legault, R. A. and A. G. Preban. 1975. Kinetics of the atmospheric corrosion of low-alloy steels in an industrial environment. *Corrosion* 31(4):117–122.
- McLain, T. E. 1992. Strength of lag-screw connections. *Am. Soc. Civil Eng. J. Struct. Eng.* 118(10):2855–2871.
- McLain, T. E. and S. Thangjitham. 1983. Bolted connection design. *Am. Soc. Civil Eng. J. Struct. Eng.* 109(8):820–835.
- Miller, E. and J. Boxall. 1987. The effectiveness of end-grain sealers in improving paint performance in softwood joinery. *Eur. J. Wood Wood Prod.* 45(2):69–74.
- Nguyen, M. N., R. H. Leicester, C.-H. Wang, and G. C. Foliente. 2011. Corrosion effects in the structural design of metal fasteners for timber construction. *Struct. Infrastruct. Eng.* DOI:10.1080/15732479.2010.546416. (Online only.)
- Rammer, D. R. 2001. Effect of moisture content on nail bearing strength. USDA Forest Service, Forest Products Laboratory, Madison, Wisconsin. 22 pp.
- Richards, M. J. 1990. Effect of CCA-C wood preservative on moisture content readings by the electronic resistance-type moisture meter. *Forest Prod. J.* 40(2):29–33.
- Short, N. R. and J. K. Dennis. 1997. Corrosion resistance of zinc-alloy coated steel in construction industry environments. *Trans. Inst. Metal Finishing* 75(2):47–52.
- Soltis, L. A., F. K. Hubbard, and T. L. Wilkinson. 1986. Bearing strength of bolted timber joints. *Am. Soc. Civil Eng. J. Struct. Eng.* 112(9):2141–2154.
- Soltis, L. A. and T. L. Wilkinson. 1987. Bolted connection design. General Technical Report FPL-GTR-54. USDA Forest Service, Forest Products Laboratory, Madison, Wisconsin.
- Wilkinson, T. L. 1993. Bolted connection design values based on European yield model. *Am. Soc. Civil Eng. J. Struct. Eng.* 119(7):2169–2186.
- Zelinka, S. L., D. Derome, and S. V. Glass. 2011. Combining a hygrothermal and corrosion model to predict corrosion of metal fasteners embedded in wood. *Build. Environ.* 46(10):2060–2068.
- Zelinka, S. L. and D. R. Rammer. 2009. Corrosion rates of fasteners in treated wood exposed to 100% relative humidity. *Am. Soc. Civil Eng. J. Mater. Civil Eng.* 21(12):758–763.
- Zelinka, S. L., D. R. Rammer, and D. S. Stone. 2008. Electrochemical corrosion testing of fasteners in wood extract. *Corrosion Sci.* 50(5):1251–1257.
- Zelinka, S. L., R. J. Sichel, and D. S. Stone. 2010. Exposure testing of fasteners in preservative treated wood: Gravimetric corrosion rates and corrosion product analyses. *Corrosion Sci.* 52(12):3943–3948.
- Zelinka, S. L. and D. S. Stone. 2010. The effect of tannins and pH on the corrosion of steel in wood extracts. *Mater. Corrosion* 62(8):739–744.
- Zelinka, S. L. and D. S. Stone. 2011. Corrosion of metals in wood: Comparing the results of a rapid test method with long-term exposure tests across six wood treatments. *Corrosion Sci.* 53(5):1708–1714.
- Zhang, X. G. 2003. Corrosion of zinc and zinc alloys. In: ASM Handbook. Vol. 13B. Corrosion: Materials. S. D. Cramer and B. S. Covino (Eds.). ASM International, Materials Park, Ohio. pp. 402–417.